



# XANES Study of Tribofilm Formation With Low Phosphorus Additive Mixtures of Phosphonium Ionic Liquid and Borate Ester

Kimaya Vyavhare<sup>1</sup>, Vibhu Sharma<sup>1</sup>, Vinay Sharma<sup>1</sup>, Ali Erdemir<sup>2</sup> and Pranesh B. Aswath<sup>1\*</sup>

<sup>1</sup> Materials Science and Engineering, University of Texas at Arlington, Arlington, TX, United States, <sup>2</sup> Department of Mechanical Engineering, Texas A&M University, College Station, TX, United States

## OPEN ACCESS

### Edited by:

Harman Khare,  
Gonzaga University, United States

### Reviewed by:

Hui Wu,  
University of Wollongong, Australia  
Liran Ma,  
Tsinghua University, China

### \*Correspondence:

Pranesh B. Aswath  
aswath@uta.edu

### Specialty section:

This article was submitted to  
Tribology,  
a section of the journal  
Frontiers in Mechanical Engineering

**Received:** 23 February 2021

**Accepted:** 06 April 2021

**Published:** 28 April 2021

### Citation:

Vyavhare K, Sharma V, Sharma V,  
Erdemir A and Aswath PB (2021)  
XANES Study of Tribofilm Formation  
With Low Phosphorus Additive  
Mixtures of Phosphonium Ionic Liquid  
and Borate Ester.  
Front. Mech. Eng. 7:671457.  
doi: 10.3389/fmech.2021.671457

The development of low phosphorus engine oils is important to minimize phosphorus-induced exhaust catalyst poisoning and resulting in harmful emissions. In this study, low phosphorus oil formulations were prepared by using an ashless additive mixture of borate ester (SB) with ionic liquid composed of a phosphonium cation and phosphate anion (P\_DEHP) at 350 and 700 ppm phosphorus. Tribological properties of this binary additive system were evaluated using a reciprocating cylinder on a flat test configuration. Favorable interaction between P\_DEHP and SB resulted in a significant reduction in friction coefficient and wear volume, in particular for P\_DEHP(700P) + SB oil blend. Time-scale analysis of tribofilm formation was determined by running the tribological experiments for 5, 15, and 60 min duration. Electrical contact resistance (ECR) results revealed that the addition of P\_DEHP at 350 ppm of phosphorus to SB at 500 ppm of boron can reduce the incubation time from 300 to 100 s for stable tribofilm formation. X-ray absorption near-edge spectroscopy (XANES) analysis of tribofilms indicates that the tribofilm mechanism for additive mixtures of P\_DEHP and SB initially involves the formation of boron oxide-based films, which later interact with phosphorus to form boron phosphates in addition to iron phosphates. Incorporation of the high amount of boron phosphates in addition to boron oxide/acid and iron phosphates in the tribofilms contributed to the improved tribological performance of P\_DEHP(700P) + SB oil. XANES results reveal that tribofilms formed due to the interaction of SB and P\_DEHP evolve to a cross-linked structure, wherein the chain length of polyphosphates is increased with the increase in rubbing time.

**Keywords:** ionic liquids, XANES, borate esters, tribofilms, tribology, lubrication, surface science, wear

## INTRODUCTION

The poisoning of automobile catalytic converters by volatile phosphorus species in the engine oil has fueled the research to develop low phosphorus engine oils by reducing or replacing the current phosphorus-containing additives (Williamson et al., 1985; Rokosz et al., 2001; Kröger et al., 2006; Zhang et al., 2017; Khare et al., 2018; Sharma et al., 2019b; Vyavhare et al., 2021b). Since 1988, the amount of phosphorus in engine oil is on a downward trajectory (Spikes, 2004), and recently the international lubricant standardization and approval committee (ILSAC) has

introduced the GF-6 performance standards which limits the phosphorus concentration in engine oils to 800 ppm maximum (Anand et al., 2015). The conventional lubricant anti-wear and antioxidant additive, zinc dialkyl dithiophosphate (ZDDP) is the main source of phosphorus in the engine oils and is known to contaminate catalytic converters, reducing its performance and service life, and increasing automotive emissions at the tailpipe (Williamson et al., 1985; Angelidis and Sklavounos, 1995; Forzatti and Lietti, 1999; Angove and Cant, 2000; Rokosz et al., 2001; Spikes, 2004; Kröger et al., 2006; Buwono et al., 2015). Additionally, ZDDP provides sulfur and zinc in the engine oil contributing to elevated levels of ash deposits and sludge formation. Considering the undesirable side-effects of existing additive chemistries and current regulations on chemical limits of phosphorus coupled with the overall objective to enhance engine efficiency and fuel economy, significant research work has been devoted to the development of novel environment-friendly (no P, S, or Zn) high-performance additives. In recent years, metal-free ashless additives, such as ionic liquids and boron-based compounds have emerged as promising candidates to partially or totally replace ZDDP without reducing the performance of conventional engine oils (Deshmukh et al., 2005; Erdemir, 2008; Lovell et al., 2010; Greco et al., 2011; Reeves et al., 2013; Shah et al., 2013; Baş and Karabacak, 2014; García et al., 2014; Qu et al., 2015; Sharma et al., 2015, 2016a,b, 2019a; González et al., 2016; Bagi et al., 2018; Vyavhare and Aswath, 2019).

The use of ionic liquids (ILs) in the field of tribology was first reported in 2001 (Ye et al., 2001) and since then an active line of research has been focused on exploiting the potential of ILs as the next generation green lubricants. ILs are synthetic molten salts formed due to weak coordinating bonds between anion and cation (Blanco et al., 2017). The unique properties of ILs like high thermal stability, non-flammability, and low volatility make them suitable for tribological applications involving severe working conditions like higher speeds, higher working temperatures, and higher mechanical stresses. Till date, ILs have been used as the base lubricants (Lu et al., 2004; Mu et al., 2005, 2008; Jiménez et al., 2006; Xia et al., 2006; Jiménez and Bermúdez, 2007; Weng et al., 2007; Kondo et al., 2012) or lubricant additives (Phillips and Zabinski, 2004; Jiménez et al., 2006; Weng et al., 2007; Jiménez and Bermúdez, 2008; González et al., 2016; Sharma et al., 2016a, 2019a; Vyavhare and Aswath, 2019). However, the practical tribological application of ILs is hindered due to problems of corrosion and limited solubility in non-polar hydrocarbon oils. In recent years, a new class of phosphonium based ILs was discovered to overcome these disadvantages. Extensive studies by Qu et al. (2012, 2014) and Yu et al. (2012) demonstrated that phosphonium–phosphinate, and phosphonium–phosphate ILs are non-corrosive, thermally stable, and oil miscible, and, more importantly, possess excellent anti-wear and anti-friction capability when used as lubricant additive in mineral base oils and fully-formulated oils. They have also shown comparable or even superior anti-wear and anti-scuffing properties of phosphonium ILs in comparison with ZDDP in PAO base oils at 1 wt.% concentration under room and elevated temperatures. Anand et al. (2015) studied the tribological performance of phosphonium ILs in engine aged fully formulated oils and proposed that addition of ILs substantially improve the service

life of used oils by forming boundary films in the presence of existing additives (like ZDDP) in the engine oil. Many studies have attributed excellent tribological properties of ILs to their tribofilm formation at the interacting metal surfaces.

Another class of environment-friendly additive is of boron based materials wherein compounds like hexagonal boron nitride (Watanabe et al., 1991; Martin et al., 1992; Mosuang and Lowther, 2002; Koskilinna et al., 2006), organic borates (Zheng et al., 1998; Philippon et al., 2011; Miller et al., 2012; Sharma et al., 2016b, 2019a), and boric acid (Erdemir et al., 1990, 1991; Erdemir, 1991; Liang and Jahanmir, 1995) are already used in lubricants as friction modifiers, corrosion inhibitors, anti-oxidants, and anti-wear additives. The excellent tribological behavior of boron compounds could be due to their strong affinities for interacting with different reactive elements. For example, boron interacts with oxygen to form  $B_2O_3$  which is highly lubricious and provides low friction (Shah et al., 2013). In addition, boron can react with interacting metal surfaces to form hard metal borides which are known to minimize wear (Shah et al., 2013). Other interesting alternative approaches to developing high-performance green lubrication is to use additive mixtures like ionic liquids with ashless dithiophosphates (Aswath et al., 2017), ionic liquids with ZDDP (Qu et al., 2012, 2014, 2015; Anand et al., 2015; Monge et al., 2015; Huang et al., 2017) or ionic liquids with nanomaterials (Li et al., 2018; Sharma et al., 2018; Vyavhare and Aswath, 2019). Considering the potential of such additive mixtures to improve friction and wear behavior of oil formulations, in this context, we have developed low phosphorus oil blends using an additive mixture of phosphonium IL and borate esters.

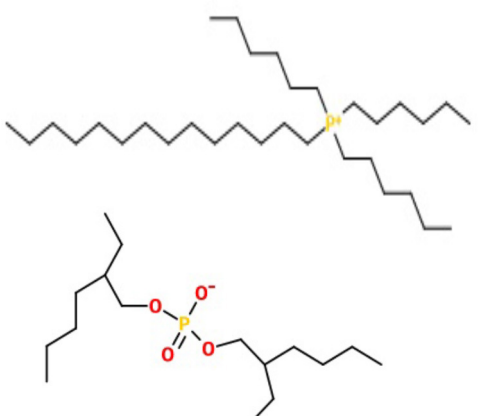
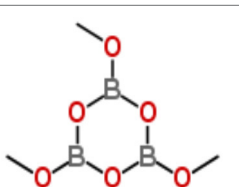
The present study is a significant extension of previously reported work on anti-wear properties of the binary ashless blend of phosphonium ILs and borate esters in group I mineral base oil (Sharma et al., 2016b). In the prior study, it was clearly demonstrated that oil formulations (with 1,000 ppm of P) containing oil-miscible phosphonium ILs and borate esters provided synergistic interaction when studied under boundary lubrication conditions. Remarkable reductions in wear volume values were observed as compared to oil containing ZDDP (Sharma et al., 2016b). In the current study, a time-scale approach is employed to understand the incubation time and mechanism of tribofilm formation for low phosphorus oils (350 and 700 ppm of P) containing phosphonium IL with borate ester. Studying the evolution of the chemistry of tribofilms with the increase in sliding time would help to elucidate the wear mechanism of anti-wear additives. For this purpose, tribofilm samples were procured from the interaction of phosphonium IL and borate ester for 5, 15, and 60 min rubbing time and characterized through electrical contact resistance (ECR) and X-ray absorption near edge spectroscopy (XANES) techniques.

## EXPERIMENTAL DETAILS

### Chemistry of Anti-wear Additives and Test Oil Formulations

**Table 1** details the chemistry of all the anti-wear additives used in this study. Low phosphorus test oils were formulated by mixing

**TABLE 1** | Molecular structure of anti-wear additives.

| Coded name | Chemical name  | Chemical structure   | Phosphorus or boron concentration |
|------------|--|--|-----------------------------------|
| P_DEHP     | Trihexyltetradecylphosphonium bis(2-ethylhexyl)phosphate |  | Phosphorus (P):<br>7.69 wt.%      |
| SB         | Trimethoxyboroxine                                       |   | Boron (B):<br>18.68 wt.%          |

trihexyltetradecylphosphonium bis(2-ethylhexyl)phosphate (P\_DEHP) IL with trimethoxyboroxine borate ester (SB) in group I base oil. P\_DEHP ionic liquid was purchased from IOLITEC Ionic Liquids Technologies Inc., details of which are available in Sharma et al. (2016a,b); Sharma et al. (2019a). SB borate ester was provided from Argonne National Laboratory. Group I base oil was purchased from a commercial vendor and was a mixture of 60 wt.% solvent neutral 150 W and 40 wt.% bright stock 90 W. The kinematic viscosity of the base oil was 10.1 mm<sup>2</sup>/s at 100°C. The phosphorus concentration in the test oils was kept at 700 and 350 ppm, while boron concentration was maintained at 500 ppm boron treat rate. Details regarding the oil formulations used in this study are shown in **Table 2**.

## Tribological Test Procedure and Characterization of Tribofilms

A High-frequency reciprocating cylinder on a flat surface test setup was used to evaluate the tribological performance of the different oils prepared in this study. The tribological testing machine was built in-house at Argonne National Lab. The 52100 hardened steel flat (14 mm × 14 mm; HRc 60–61; Sa 8 nm) and cylinder (4 mm × 6 mm; HRc 60–61) were used in this study. The load was applied using a pneumatic pressure unit to exert initial Hertzian contact pressure of 500 MPa. Experiments were performed at 0.06 m/s reciprocation speed at 100°C. The stroke length was 6 mm. To better understand tribofilm forming time and mechanism due to interaction of ionic liquid and borate ester at the interface, tribological tests were performed at different durations of 5, 10, and 60 min. Experiments were repeated twice to ensure repeatability and consistency in the results.

**TABLE 2** | Overview of low phosphorus test oil formulations prepared using P\_DEHP and SB anti-wear additives.

| S. No. | Coded name        | Details of test oil formulations  |
|--------|-------------------|---|
| 1      | SB                | Group I base oil + SB (added at 500 ppm boron treat rate)   |
| 2      | P_DEHP(350P) + SB | Group I base oil + P_DEHP (added at 350 ppm phosphorus treat rate) + SB (added at 500 ppm boron treat rate) |
| 3      | P_DEHP(700P) + SB | Group I base oil + P_DEHP (added at 700 ppm phosphorus treat rate) + SB (added at 500 ppm boron treat rate) |

Tribometer was also equipped with electric contact resistance (ECR) measurement circuit, wherein the potential of 100 mV was applied between counter steel surfaces of the cylinder and flat. The voltage drop across the counter surfaces was collected *in-situ* during the test to gain insight into the incubation time for tribofilm formation at the tribological interfaces. All test specimens were cleaned before the test using Stoddard solution followed by isopropanol and acetone to completely remove any oil and dust present on the surfaces. Tests were conducted by using 15 μl of prepared oil formulations to lubricate the interface between flat and cylinder test specimens. After the completion of the test, specimens were cleaned with heptane and isopropanol and then saved for characterization by submerging in additive-free polyalphaolefin (PAO) oil.

Friction forces were recorded *in-situ* through strain gauge load cell and coefficient of friction data was acquired using the

DasyLab software. To conduct wear performance assessment, wear surfaces developed on the cylinders were examined under an optical microscope and a 3D optical interferometer. An optical image of the cylindrical test specimen was used to measure wear scar width at nine locations and an average of nine wear width measurements was used to calculate the wear volume of each cylinder. Wear surface (center/edge region) developed on flat steel specimen was characterized using the surface-sensitive technique, XANES spectroscopy to understand the chemical nature of tribofilms formed *in-situ* at the sliding surfaces. XANES spectra were obtained at the Canadian Light Source synchrotron facility in Saskatoon Canada. The phosphorus L-edge (P L-edge) and Boron K edge (B K-edge) spectra were collected at VLS-PGM (variable line spacing plane grating monochromator) beam station that operates at the energy range of 5.5–250 eV with a photon resolution of more than 10,000 E/ $\Delta E$ . All the spectra were collected using a 100  $\mu\text{m}$   $\times$  100  $\mu\text{m}$  photon beam spot size.

## RESULTS AND DISCUSSION

### Evaluation of Coefficient of Friction and Wear Volume

The coefficient of friction (CoF) obtained for different oil blends at 5 min (black line), 15 min (red line), and 60 min (blue line) tests are plotted in **Figure 1**. All three oil formulations show overall stable frictional behavior. A small variance is observed in the CoF value for 5 min tests compared to 60 min tests for all oil formulations. This could be attributed to the original surface roughness of the test specimen. In the initial stages of the test, the frictional resistance between the counter surfaces is dominated by the original surface roughness which could vary a little while preparing the sample. Once the initial surface asperities are removed and stable tribofilms form on the counter surface, a stable friction response is observed. Additionally, CoF values for initial 5 min of 15 and 60 min tests appear to be similar suggesting the consistency in the additive performance. A careful comparison of 60 min COF profiles hints at almost similar steady-state friction values for all three formulations. An average coefficient of friction was calculated for 60 min tests and is plotted in **Figure 2**. Oil formulation containing only SB exhibits the highest CoF value while binary additive blends containing P\_DEHP and SB results in lower CoF. In addition, P\_DEHP(700P)+SB exhibits lower CoF compared to P\_DEHP(350P)+SB.

Optical images of the wear scar developed on cylinders and flat after 1-h tribological tests are shown in **Figure 3**. Wear characteristics on both cylinder and flat lubricated with P\_DEHP(700P)+SB appears to be better than SB and P\_DEHP(350P)+SB oils. Worn surface lubricated with SB exhibits deeper scratches in the direction of sliding and regions of abrasive wear with high surface roughness covered with small patches of tribofilms. The optical image obtained for P\_DEHP(350P)+SB lubricated wear surface shows signs of mild polishing wear with several scratches aligned in the sliding direction over the smooth surface and few regions covered with small patches of protective tribofilms. The wear scar

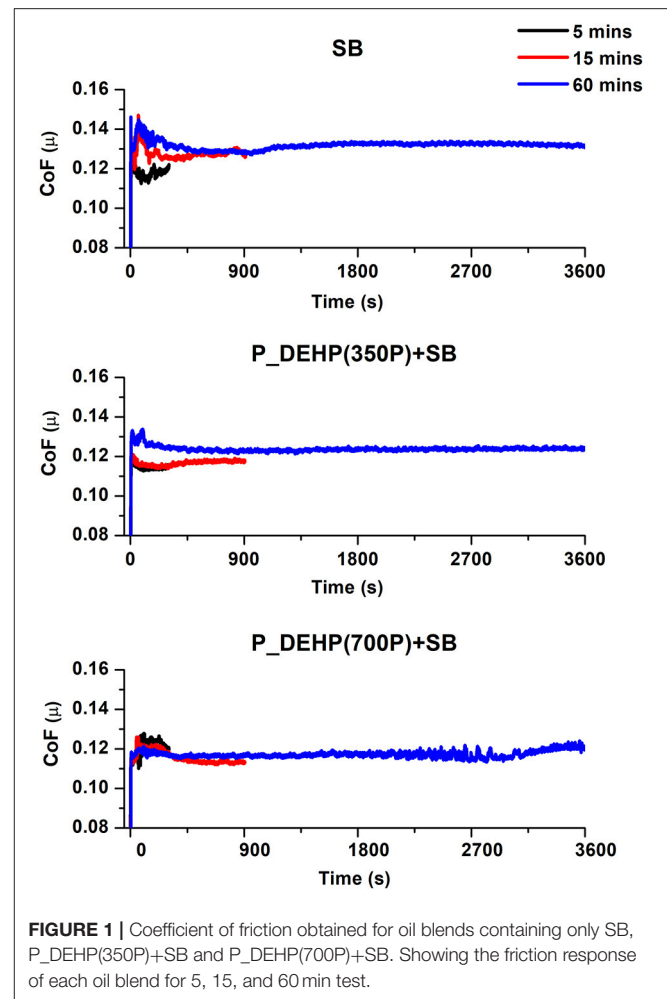
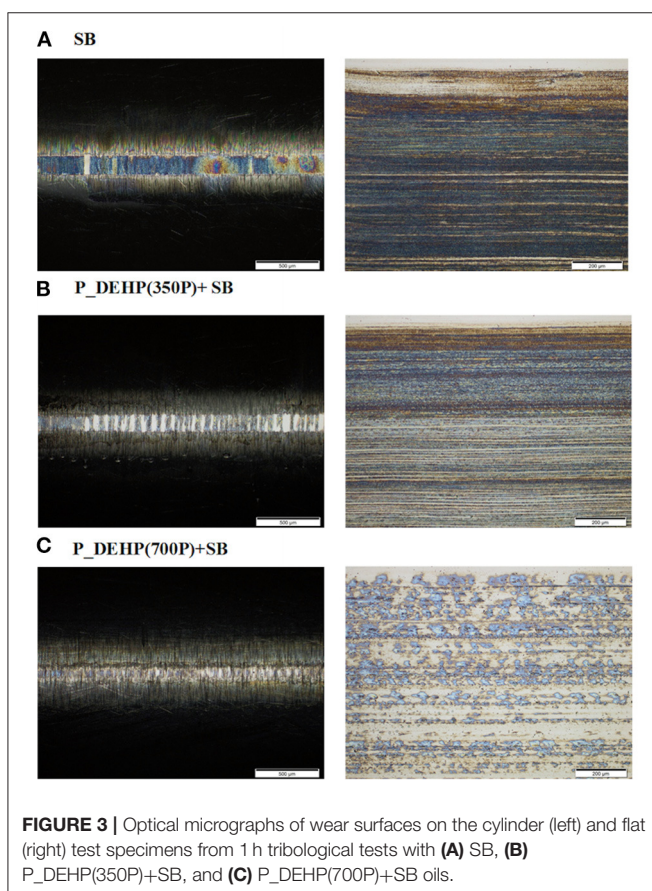
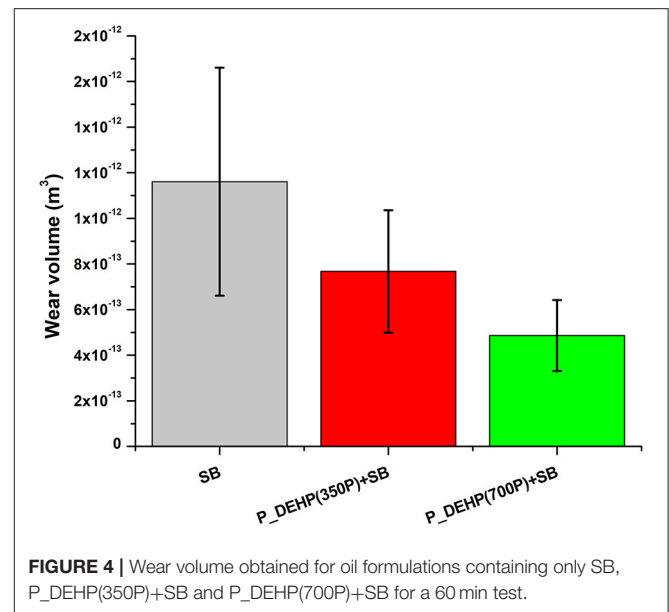
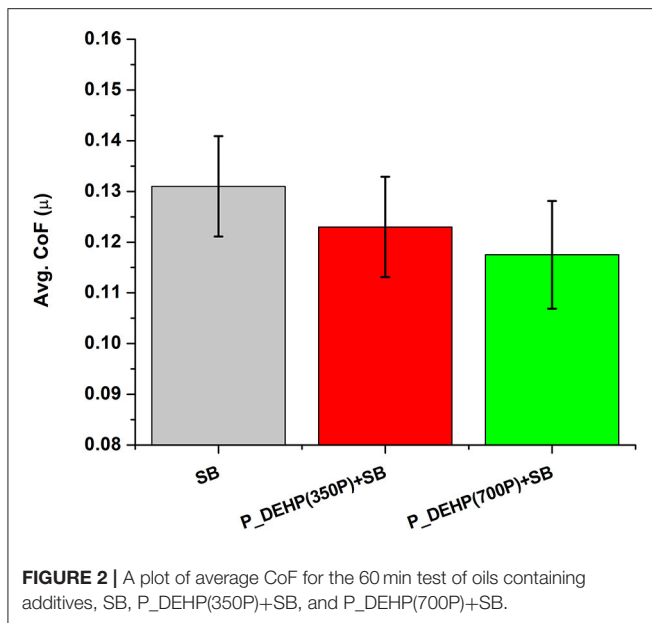


**FIGURE 1** | Coefficient of friction obtained for oil blends containing only SB, P\_DEHP(350P)+SB and P\_DEHP(700P)+SB. Showing the friction response of each oil blend for 5, 15, and 60 min test.

generated on a flat specimen lubricated with P\_DEHP(700P)+SB appears to be smooth and exhibits the presence of patchy protective tribofilms over the worn surface with mild scratching. Importantly, the optical image of P\_DEHP(700P)+SB wear scar exhibits better tribofilm coverage with patch sizes that are larger and continuous than what is seen in SB and P\_DEHP(350P)+SB. This indicates that P\_DEHP(700P)+SB lubricant provided better wear protection than SB and P\_DEHP(350P)+SB through the formation of protective tribofilms at the tribological interface.

Wear volume calculated for all oil formulations after 60 min is presented in **Figure 4**. Wear scar width for 5 and 15 min test was very low and precise measurements could not be made, hence are not presented here. Error bars in **Figure 4** represent the standard deviation between wear volume measured for two repeat tests. Borate ester when used by itself exhibits higher wear volume compared to formulations containing additive mixtures of P\_DEHP and SB. Moreover, the effect of phosphorus content in the oil blend can also be seen in **Figure 4**. The binary mixtures of P\_DEHP+SB exhibited improvement in the wear protection when the phosphorus treat rate was increased from 350 to 700 ppm. The addition of phosphorus from P\_DEHP to the SB at



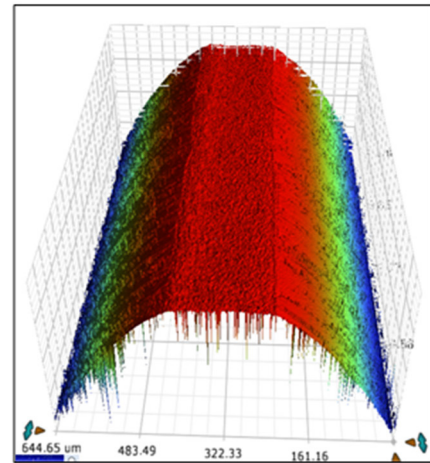
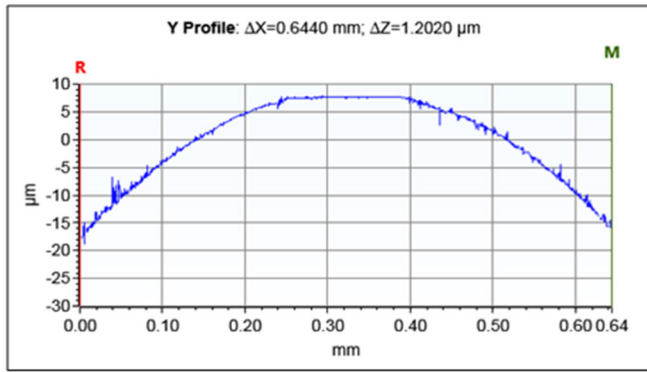
350P ppm shows improvement in the wear protection which is further increased by adding P\_DEHP at 700P ppm to SB. **Figure 5** shows optical profilometry 2D images of the wear scar

profile at the center of the cylinders and 3D images of the area of contact on the cylinders after tribological tests. The cylinder surface for SB reveals severe wear as the 2D profile is virtually flat at the center. The improved wear protection with the additive mixture of borate ester, SB, and P\_DEHP ionic liquid at 700 ppm of P is visually evident in the 3D profilometry images.

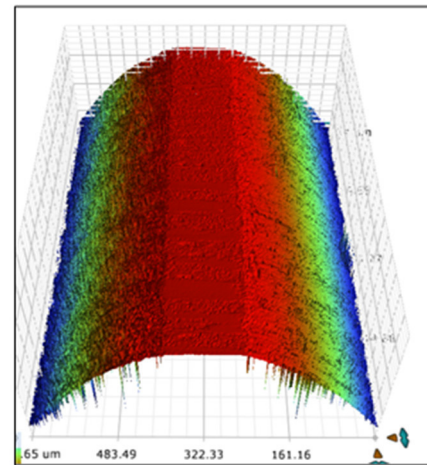
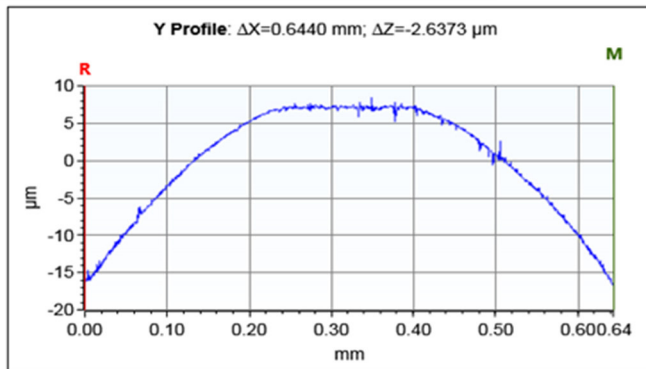
### Analysis of Tribofilms Formation Using ECR

ECR data acquired for all oil formulations during the 5 min (black), 15 min (red), and 60 min (blue) test is shown in **Figure 6**. Graphs in **Figure 6** represent voltage drop values measured as a function of test time. Non-zero voltage drop value is indicative of the formation of non-conductive glassy tribofilms and voltage drop close to zero mV suggests no film formation between the counter surfaces. Five minutes test with a formulation containing only SB does not show potential build-up except the first point which could originate due to separation of counter surfaces from oil. Once the test started voltage drop value becomes near zero suggesting no tribofilms were formed within 5 min. Both 15 and 60 min test shows the potential build-up to 100 mV at ~300 s after the start of the test. These results indicate that the incubation time for tribofilm formation for borate ester (SB) additive is ~300 s. After ~300 s, both 15 and 60 min test show voltage drop value which periodically vary between 0 and 100 mV until ~900 s test time. This corresponds to the film formation which is sacrificial in nature. In this test duration (~300 to ~900 s), the film formation rate is similar to the film removal rate under constant shearing forces. After ~900 s, a more stable voltage drop is observed, and the voltage drop value varies between ~50 and 100 mV till ~2,700 s test time. In this test duration, most voltage drop values remained close to 100 mV indicating stable and effective film formation. After ~2,700 s voltage drop value starts to decrease till the end of the test i.e., 3,600 s. ECR data acquired

**A SB**



**B P\_DEHP(350P)+SB**



**C P\_DEHP(700P)+SB**

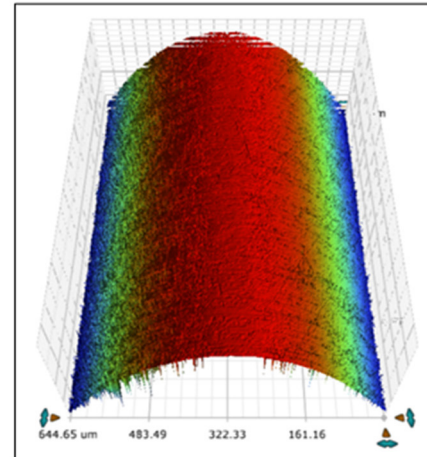
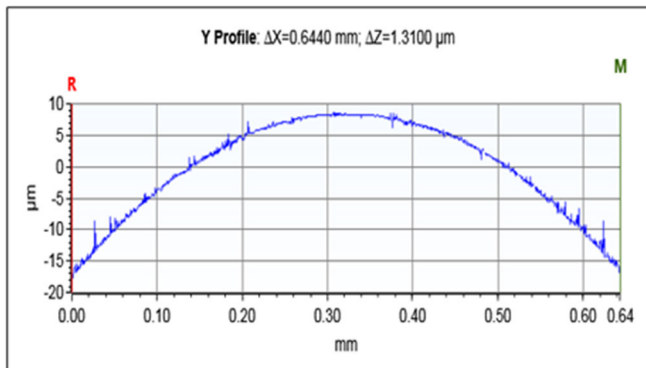


**FIGURE 5 |** Optical profilometry images of the cylinders represented in 2D (left) at the center region of the cylinder and the 3D representation of the wear scar developed after 1 h **(A)** SB, **(B)** P\_DEHP(350P)+SB, **(C)** P\_DEHP(700P)+SB tribological tests.

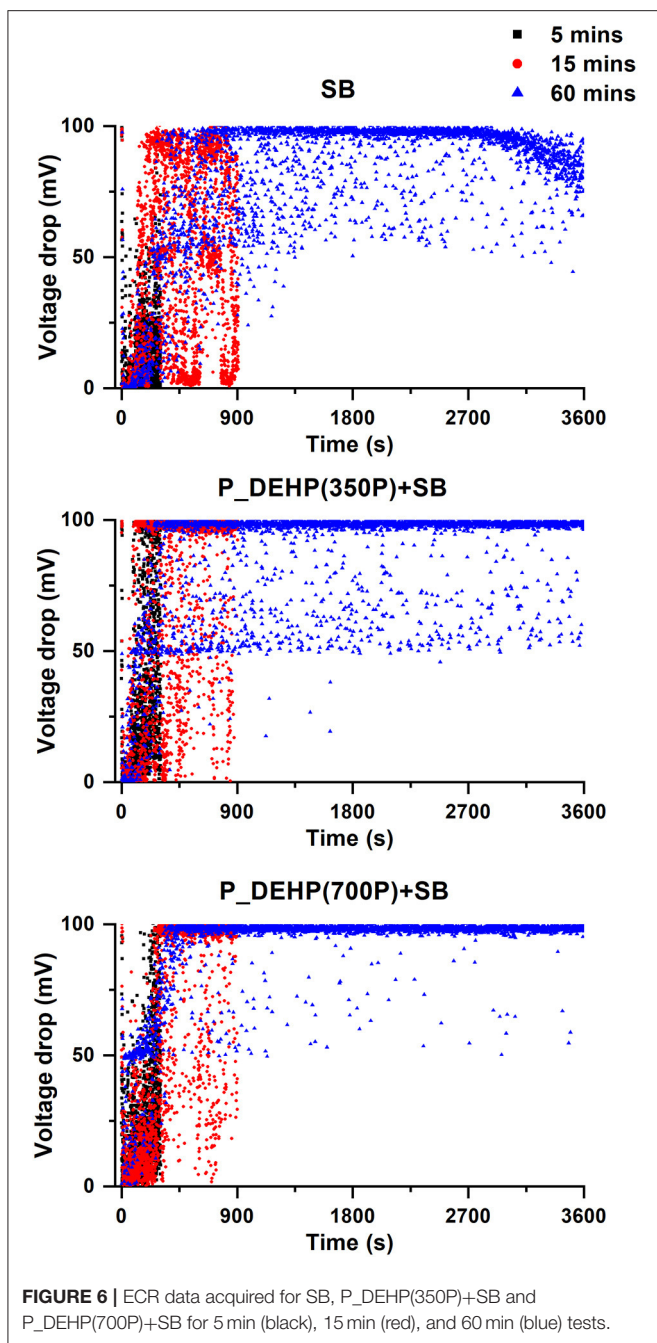


**FIGURE 6** | ECR data acquired for SB, P\_DEHP(350P)+SB and P\_DEHP(700P)+SB for 5 min (black), 15 min (red), and 60 min (blue) tests.

for the test run under P\_DEHP(350P)+SB lubrication shows a relatively small incubation time for tribofilm formation. Voltage drop starts to form as early as  $\sim 100$  s from the beginning of the 5, 15, and 60 min tests. After  $\sim 100$  s, voltage drop values vary between 50 and 100 mV. These results indicate that the addition of phosphorus from P\_DEHP at 350P ppm to SB promotes tribofilm formation in a very short time and once the films are formed film formation rate is higher than film removal under shearing, thus the voltage drop does not go back to 0 mV and stays between 50 and 100 mV. In the case of P\_DEHP(700P)+SB,

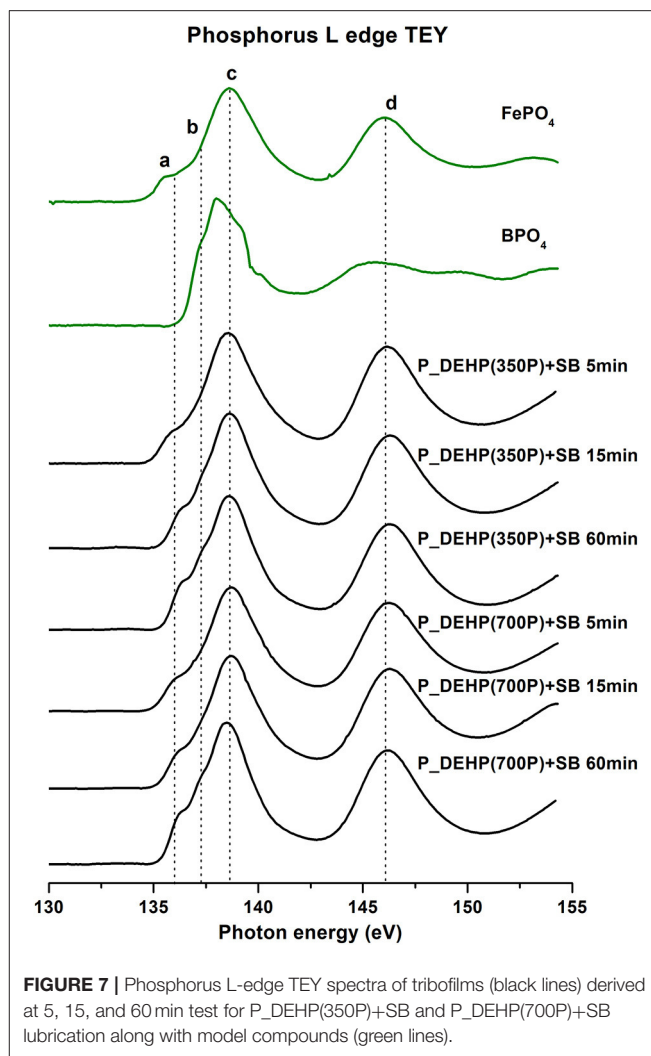


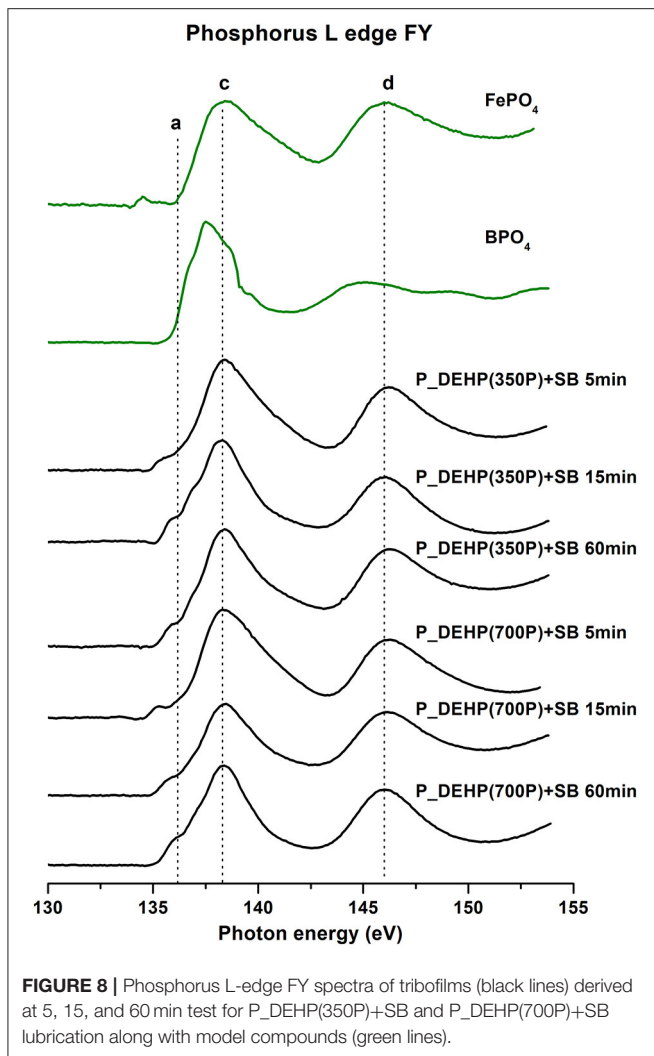
**FIGURE 7** | Phosphorus L-edge TEY spectra of tribofilms (black lines) derived at 5, 15, and 60 min test for P\_DEHP(350P)+SB and P\_DEHP(700P)+SB lubrication along with model compounds (green lines).

voltage drop starts to build up as early as the test starts however, till  $\sim 300$  s of the test, the film removal rate is higher than film formation hence the voltage drop varies between 0 and 50 mV. After  $\sim 300$  s, voltage drop value reached 100 mV indicative of stable film formation. The voltage drop value remains close to 100 mV for the rest of the test duration except at few points where voltage drop falls to 50 mV. These observations suggest that the interaction of phosphonium ionic liquid (P\_DEHP) with borate ester (SB) reduces the incubation time for tribofilm formation as well as results in more stable and effective film formation. The amount of phosphorus also determines the effectiveness of the tribofilms. The addition of P\_DEHP at 700P ppm to SB results in more effective tribofilm formation than P\_DEHP(350P)+SB.

## Chemical Properties of Tribofilms Using XANES

### Phosphorus Characterization (P $L_{2,3}$ -Edge)

Phosphorus L-edge TEY and FY spectra of wear samples derived from 5, 15, and 60 min tests with low phosphorus oil blends containing P\_DEHP at 350P ppm/700P ppm and SB at 500B



ppm is illustrated in **Figures 7, 8**, respectively. Phosphorus L-edge spectra are plotted in black lines and are compared with model compounds plotted in green lines. **Figure 7** shows the P L-edge TEY spectra which offers chemical information of local coordination of phosphorus from near-surface region i.e., ~5–10 nm (Suominen Fuller et al., 2000). The absorption peak observed on P L-edge TEY spectra is labeled as peak **a**, **b**, **c**, and **d**. Peak **d** is a characteristic shape resonance peak owing to 2p to 3d transitions (Li et al., 1994) and represents phosphate coordination irrespective of the cation associated with it. The presence of peak **d** in tribofilms spectra indicates that phosphorus is primarily present as phosphate species in the tribofilms. In addition, the photon energy of pre-edge shoulders peaks **a** and **b** and a main absorption edge peak **c** from the tribofilms spectra closely matches with FePO<sub>4</sub> model compound spectra.

Similarly, the tribofilms P L-edge FY spectra (shown in **Figure 8**) offer chemical information from the bulk of the sample up to 50–60 nm (Suominen Fuller et al., 2000; Nicholls et al., 2007) also exhibited spectral features matching with the FePO<sub>4</sub> model compound. This confirms that tribofilms derived from

P\_DEHP (350P/700P)+SB lubrication are primarily composed of FePO<sub>4</sub> chemistry. The main absorption edge from the P L-edge spectra of the BPO<sub>4</sub> model compound was not clearly resolved in the P L-edge spectra of tribofilms. Here, we can speculate that since the availability of Fe cation (from the substrate) is much higher than B (added at 500 ppm) at the tribological contacts, the likelihood for FePO<sub>4</sub> formation is much higher than BPO<sub>4</sub> in the tribofilms. Hence when probing the P L-edge, the tribofilms spectra get influenced by the more dominantly present species i.e., FePO<sub>4</sub> chemistry which might result in the suppression of spectral features of BPO<sub>4</sub> chemistry. To effectively detect the BPO<sub>4</sub> chemistry in the tribofilms, B K-edge spectra were acquired and discussed in the next section [Boron Characterization (B K-Edge)].

In order to gain insight into the effect of rubbing time and phosphorus concentration on the formation and composition of tribofilms, the extent of phosphate film polymerization was analyzed using the peak **a** to peak **c** ratio from P L-edge TEY and FY spectra of tribofilms. Previous studies have suggested that **a/c** ratio below 0.3 corresponds to short-chain phosphate polymerization and **a/c** ratio above 0.6 indicate long-chain phosphate formations (Yin et al., 1995; Li et al., 2007; Kim et al., 2011; Vyavhare et al., 2019; Cebe et al., 2020). The **a/c** ratio of tribofilms formed at 5, 15, and 60 min test for oils containing P\_DEHP(350P)+SB and P\_DEHP(700P)+SB is measured and plotted in **Figure 9**. P L-edge TEY **a/c** ratio is presented as a green bar and P L-edge FY **a/c** ratio in blue bars. The **a/c** ratio acquired from TEY spectra exhibits a higher value in comparison with FY for each test suggesting that at the near-surface region, a higher degree of polymerization had occurred than in the bulk of the tribofilms in all cases. In all cases, short-chain phosphate film formation has been observed since the maximum **a/c** ratio measured is 0.3 [P\_DEHP(350P)+SB 60 min test and P\_DEHP(700P)+SB 60 min test]. The **a/c** ratio is found to be increasing with increasing rubbing time/ test time. In the case of P\_DEHP(350P)+SB TEY/FY, the **a/c** ratio increases from 0.2/0.09 to 0.25/0.14 and 0.3/0.19 for 5, 15, and 60 min test, respectively. Similarly, P\_DEHP(700P)+SB TEY/FY also shows an increase in the **a/c** ratio with rubbing time both at near-surface (TEY) and in the bulk (FY). These results indicate that the tribofilms derived from P\_DEHP(350P/700P)+SB results in layered phosphate films where the surface (TEY) of the films is composed of relatively longer chain phosphate films than the bulk (FY) of the tribofilms.

### Boron Characterization (B K-Edge)

B K-edge TEY and FY spectra of tribofilms derived from SB, P\_DEHP(350P)+SB, and P\_DEHP(700P)+SB for 5, 15, and 60 min test are plotted in **Figures 10, 11**, respectively. The local coordination of boron in the tribofilms is identified by comparing the acquired B K-edge spectra with model compounds, trigonal boron (B<sub>2</sub>O<sub>3</sub>) and tetrahedral boron (BPO<sub>4</sub>). In **Figures 10, 11**, the trigonal boron peak for B<sub>2</sub>O<sub>3</sub> is labeled as peak **a** (194.1 eV) and the tetrahedral boron peak for BPO<sub>4</sub> is identified as peak **b** (198.4 eV). Zhang et al. (2004) reported that peak **a** originates from the p<sub>2s</sub> from phosphate structure. B K-edge TEY and FY spectra of SB-derived tribofilms for 5,



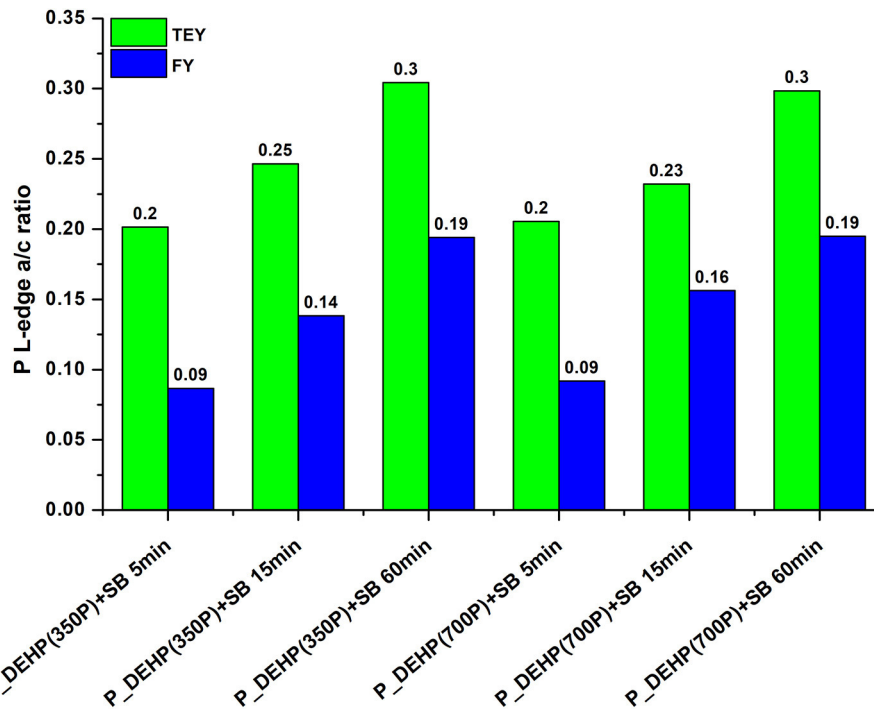


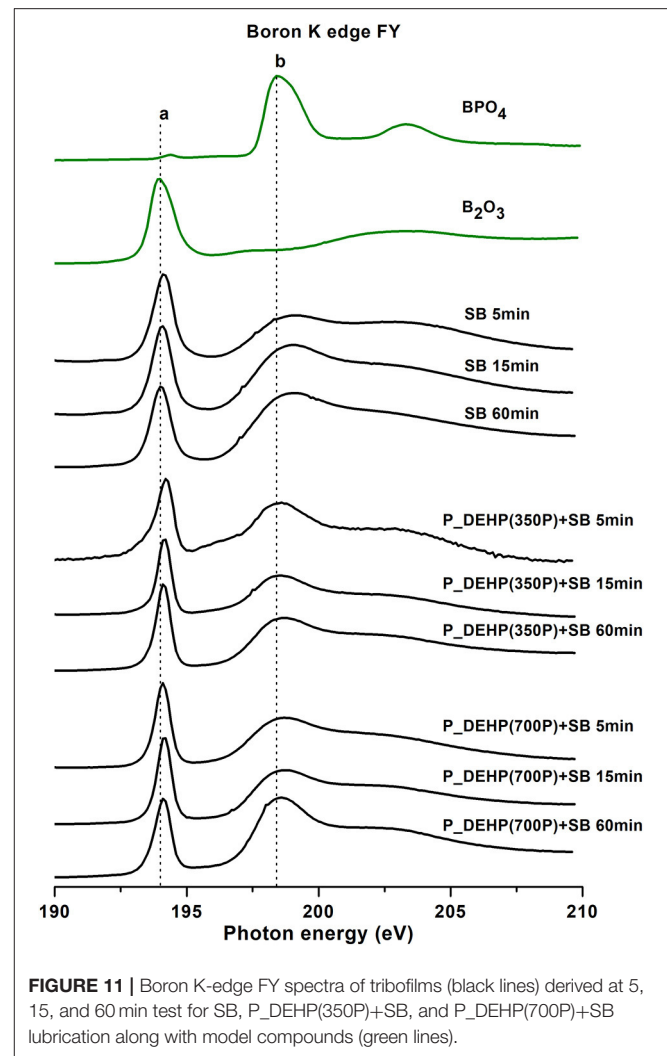
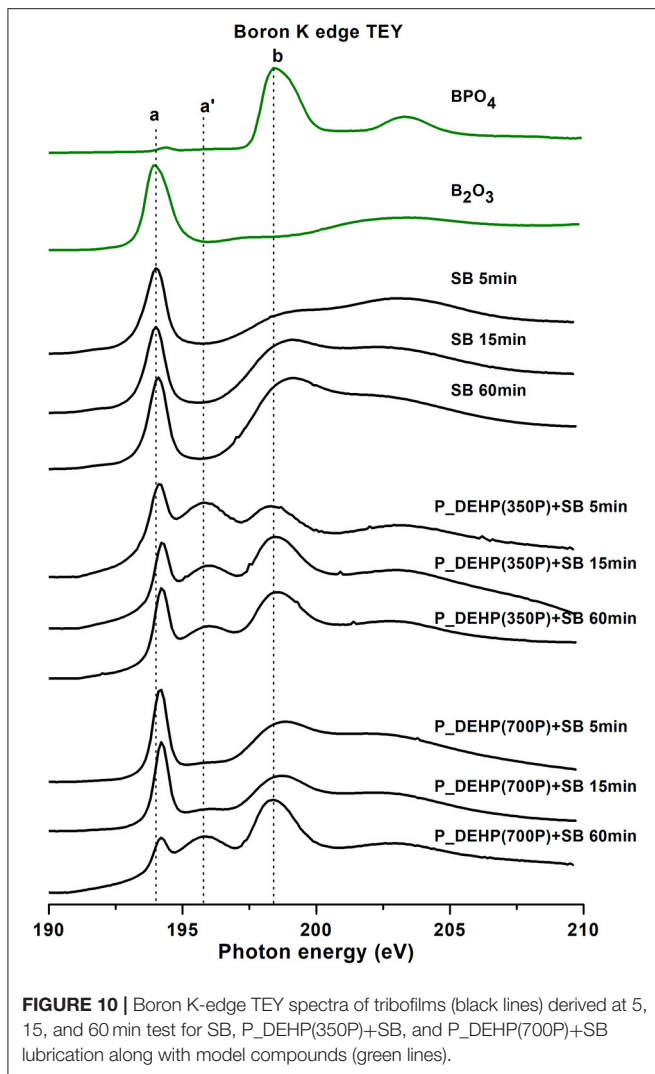
**FIGURE 9** | P L-edge a/c ratio measured for tribofilms formed using P\_DEHP(350P)+SB and P\_DEHP(700P)+SB at 5, 15, and 60 min test.

15, and 60 min tests exhibit peak **a** indicating that boron is primarily present as trigonal boron as  $B_2O_3$ . Detection of an unresolved peak at a photon energy of 199 eV (close to peak **b**) in both TEY and FY spectra indicates that under the thermo-mechanical shearing partial transformation of trigonal boron to tetrahedral boron may have occurred. In an earlier study, Zhang et al. (2004) also reported transformation of trigonal coordination to tetrahedral coordination in boron in the tribofilms upon rubbing.

B K-edge TEY and FY spectra for P\_DEHP(350P)+SB derived tribofilms exhibit two absorption edges labeled as peak **a** and peak **b**. Comparing with the model compound spectra, the presence of peak **a** at a photon energy of 194.1 eV suggests that boron in these tribofilms is trigonal boron species i.e.,  $B_2O_3$ . In addition, the presence of much-resolved peak **b** at 198.4 eV aligned with peak **b** of the  $BPO_4$  model compound suggests that to some extent boron is also present as boron phosphate. Peak **a** at the photon energy of 195.78 eV is present in the TEY spectra and not in the FY spectra. Here, peak **a** is attributed to the presence of  $FePO_4$  films on the surface (TEY), which were also identified through P L-edge results (in an earlier section). It is important to note that in TEY spectra intensity of peak **a** decreases while the intensity of peak **b** increases with the increase in rubbing time. This observation hints at the interaction of boron species with already formed  $FePO_4$  films and/ or ionic liquid to form more boron phosphate on the surface with the increase in rubbing time. Similarly, in the case of P\_DEHP(700P)+SB, for 5 and 15 min rubbing time the boron is mostly present as trigonal boron ( $B_2O_3$ ) and to less extent as tetrahedral boron.

However, with the increase in rubbing time to 60 min dominant boron chemistry in the surface (TEY) appears to be associated with tetrahedral boron, primarily as boron phosphate (exact aligned peak **b** at 198.4 eV) and to small proportion as trigonal boron ( $B_2O_3$ ). Both FY spectra of P\_DEHP(350P)+SB and P\_DEHP(700P)+SB indicate that boron is present as trigonal boron ( $B_2O_3$ ) and tetrahedral boron ( $BPO_4$ ) in the bulk of these tribofilms. However, in this case, P\_DEHP(350P)+SB blend with 60 min rubbing time exhibits the strong intensity of peak **a** as opposed to peak **b**, while P\_DEHP(700P)+SB blend 60 min test shows the higher intensity of peak **b** than peak **a**. These results suggest that high concentration of P\_DEHP (700 ppm of P) in the lubrication largely interacted with SB to form  $BPO_4$  films in both bulk and surface of the tribofilms formed during 60 min of rubbing time.

Moreover, we can see the change in the ratio of boron phosphate to boron oxide with the rubbing in **Figure 12**. The peak intensity of peak **b** increases from 5 to 60 min rubbing time. The ratio of  $BPO_4$  to  $B_2O_3$  is higher in TEY compared to FY, suggesting the boron in the bulk of the tribofilms is dominantly present as  $B_2O_3$  while  $BPO_4$  contribution increases at near-surface region. B K-edge TEY and FY spectra of P\_DEHP (700P)+SB for 60 min test exhibit the highest ratio of  $BPO_4$  to  $B_2O_3$ . We can hypothesize that during the rubbing test boron from borate ester first arrive at counter surfaces and forms  $B_2O_3$  tribofilms which later interact with phosphorus from P\_DEHP ionic liquid and/  $FePO_4$  films and form  $BPO_4$  which enhances the crosslinking between phosphate film networks.

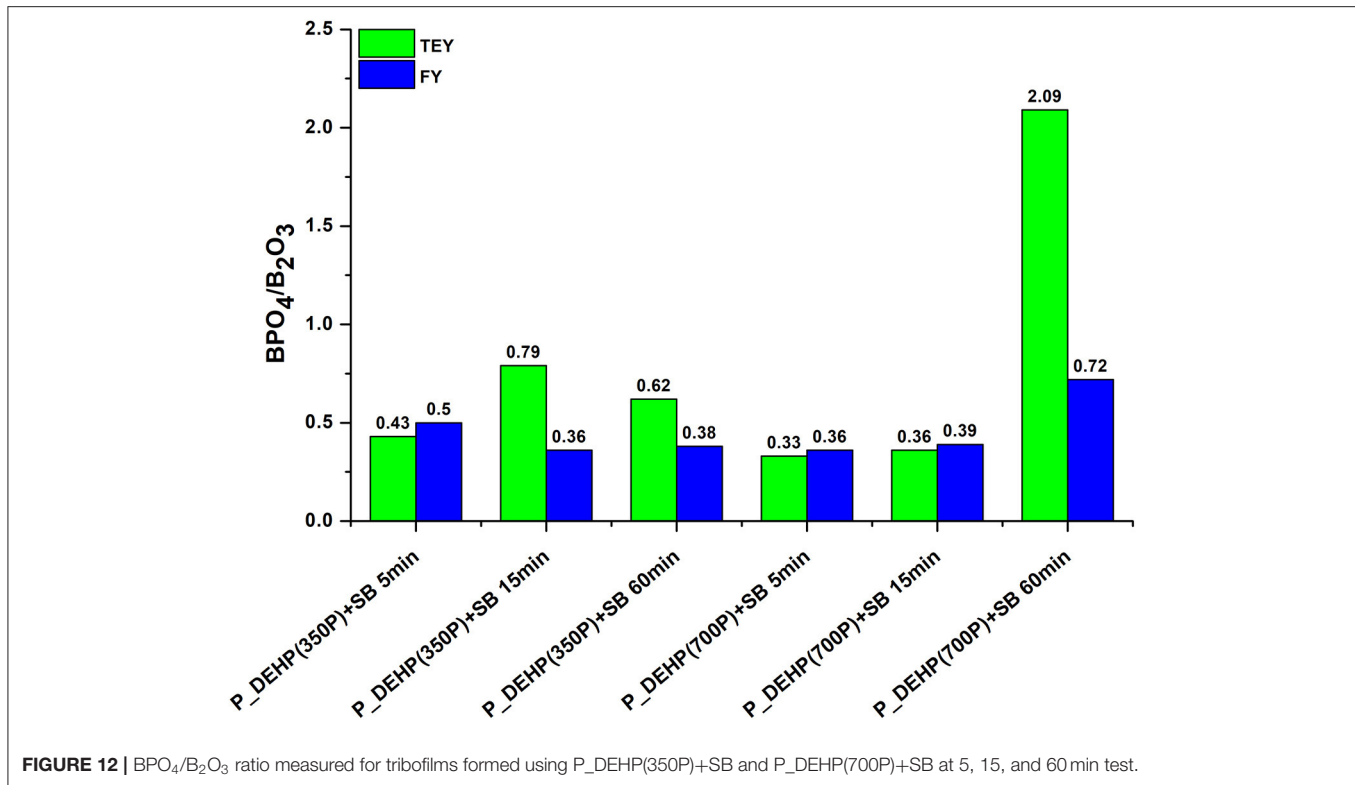


## Tribofilm Formation and Anti-wear Mechanism

Interfacial tribofilms primarily control the wear characteristics of the sliding surfaces operating under mixed to boundary lubrication regime. Extensive surface characterization techniques have been used to study physical and chemical properties of tribofilms formed from phosphorus-containing anti-wear additives like ZDDP and IL. For example, Ramoun et al. and Bohoon et al. used scanning electron microscopy (SEM) with focused ion beam (FIB), Auger electron spectroscopy, XANES, and nano-indentation techniques to evaluate chemical and physical properties of ZDDP derived tribofilms (Mourhatch, 2009; Kim et al., 2010, 2011, 2017; Mourhatch and Aswath, 2011). They reported that 100–200 nm thick tribofilms are grown from bottom to top on steel substrate in chemically varying layered structures, wherein the top layer is enriched with zinc and iron phosphates. Qu et al. and Zhou et al. using transmission electron microscopy (TEM) and scanning tunneling electron microscopy (STEM) studied nanostructure and compositional

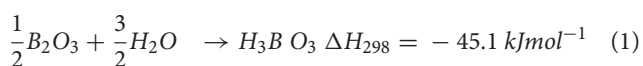
characteristics of IL tribofilms and proposed that ILs form 120–180 nm thick amorphous tribofilms via multi-step tribofilm forming mechanism including thermally activated chemical reactions at sheared metallic contacts (Qu et al., 2012; Zhou et al., 2017). In this context, our previous study (Sharma et al., 2016b, 2019a) with Group I mineral oil and fully formulated oil containing phosphonium IL (P-DEHP) examined morphological and topographical characteristics of tribofilms using scanning probe microscopy (SPM) and SEM. 3D images of the wear scar recorded using SPM revealed presence of ~80 nm thick tribofilms with patchy morphology.

This study using ECR and XANES confirms the ability of borate esters to interact chemically with phosphonium IL to form thick tribofilms and improve anti-wear performance under boundary lubrication conditions. Here, ECR results exhibited that the SB by itself forms tribofilms at a slower rate, however, the addition of P-DEHP to SB accelerated the formation of their tribofilms. It can be proposed that the additional phosphorus chemistry provided through P-DEHP promoted the stable formation of protective tribofilms at a relatively faster



rate than SB. Furthermore, the presence of phosphorus and boron chemistry in the case of P\_DEHP(700P)+SB boosted the thickness of tribofilm patches as illustrated in **Figure 3**. Formation of stable and thick tribofilms at the early-stage of sliding (~100 s) could have aided to distribute applied contact pressure and sacrificially cushion shear stresses at the tribological interface to effectively prevent wear.

XANES results confirmed that the interaction between P\_DEHP and SB additives resulted in the formation of FePO<sub>4</sub>, B<sub>2</sub>O<sub>3</sub>, and BPO<sub>4</sub> tribochemical films on the rubbed surfaces. The P L-edge spectra primarily exhibited FePO<sub>4</sub> formation suggesting that P\_DEHP IL reacts with the nascent Fe surface to form FePO<sub>4</sub>. B K-edge spectra identified the association of boron with trigonal coordination as B<sub>2</sub>O<sub>3</sub> and with tetrahedral coordination as BPO<sub>4</sub>. The authors hypothesize that under the thermo-mechanical shearing, borate esters (SB) form decomposition by-products of B<sub>2</sub>O<sub>3</sub> on the counter surfaces during the initial stage of the test. However, since the tribological experiments were run in ambient air (relative humidity ≈50%), B<sub>2</sub>O<sub>3</sub> can also hydrolyze to form boric acid (H<sub>3</sub>BO<sub>3</sub>). Erdemir et al. (1990) studied the lubrication mechanism of boron chemistry and reported that B<sub>2</sub>O<sub>3</sub> transforms into H<sub>3</sub>BO<sub>3</sub> at the tribological contacts following the reaction (1).



Additionally, B K-edge spectra of tribofilms do not show a characteristic peak of FeB at a photon energy of around 191.5 eV

(Sharma et al., 2016b) and thus, confirm no interaction of boron chemistry with the nascent Fe surface.

On the other hand, the tribochemical reaction of ionic liquids and/or their decomposition products with the nascent Fe surfaces and/or wear debris at the interface has resulted in the formation of protective FePO<sub>4</sub> films. The primary source of phosphorus for physiochemical reaction can be from the phosphate anion as it is easier for the phosphate anion to lose alkyls and react with the nascent metal surface (Somers et al., 2013; Qu et al., 2014; Zhou et al., 2014) to form iron phosphates in opposed to the phosphonium cation. However, the contribution from the phosphonium cation can't be completely ruled out. Our previous work on oil miscible phosphonium cation and non-phosphorus anion-based ionic liquid has shown the formation of iron phosphate films due to complex decomposition and/or oxidation of phosphonium cations and reaction of these decomposition products with the underlying nascent Fe substrate (Sharma et al., 2016a). Besides these compounds, the B K-edge spectra of the binary additive mixture P\_DEHP+SB also exhibited the formation of the BPO<sub>4</sub> compound. From **Figure 10**, it was also noticed that with rubbing time, BPO<sub>4</sub> formation increases in the tribofilms relative to B<sub>2</sub>O<sub>3</sub>. Thus, it can be postulated that under the thermo-mechanical shearing, BPO<sub>4</sub> forms at the expense of B<sub>2</sub>O<sub>3</sub> due to the availability of phosphorus either from the original P\_DEHP IL or from FePO<sub>4</sub> films.

XANES P L-edge indicated that the tribofilms formed with P\_DEHP(350P/700P)+SB contains relatively longer chain-length phosphates in the near-surface region than the bulk of the tribofilms. Earlier studies have shown that longer

chain phosphates yield better tribological properties and are generally considered to be more beneficial (Bancroft et al., 1997; Mosey et al., 2006; Sharma et al., 2015; Vyavhare et al., 2021a,b,c, Vyavhare et al., 2021). Additionally, XANES results indicated that the chain length of phosphates increases with the rubbing time. It can be proposed that the high pressure and temperature experienced due to extended rubbing time from 5 to 60 min could have induced cross-linking of loosely interacting iron phosphates molecules into a chemically connected network. Additionally, as discussed earlier with increased rubbing, the concentration of BPO<sub>4</sub> has also increased in the tribofilm. Boron exhibits variable co-ordination number, which allows it to act as both glass former and cross-linking agent (Mosey et al., 2006), and therefore, here increase in the formation of BPO<sub>4</sub> might have contributed to the increase in the overall chain length of phosphates in the tribofilms. Overall, it is evident from this study that the tribo-chemical reaction of SB and P\_DEHP reduces the incubation time to form protective tribofilms and promotes the formation of cross-linked glassy phosphates with the increased sliding time that lead to a corresponding improvement in anti-wear properties.

## CONCLUSIONS

Oils with additive mixtures of borate esters with phosphonium IL at a phosphorus treat rate of 350 and 700 ppm were developed. Antiwear properties measured for these oil formulations on a cylinder-on-flat contact under pure sliding revealed noticeable improvement in wear protection for binary additive mixtures of SB with P\_DEHP compared to SB alone. Phosphorus treat rate can also be combined with the wear outcomes since P\_DEHP(700P)+SB resulted in the lowest wear volume compared to P\_DEHP(350P)+SB, while oil blend SB with no P exhibited the highest wear volume.

## REFERENCES

- Anand, M., Had, M., Viesca, J. L., Thomas, B., Battez, A. H., and Austen, S. (2015). Ionic liquids as tribological performance improving additive for in-service and used fully-formulated diesel engine lubricants. *Wear* 335, 67–74. doi: 10.1016/j.wear.2015.01.055
- Angelidis, T. N., and Sklavounos, S. A. (1995). A SEM-EDS study of new and used automotive catalysts. *Appl. Catal. A Gen.* 133, 121–132. doi: 10.1016/0926-860X(95)00165-4
- Angove, D. E., and Cant, N. W. (2000). Position dependent phenomena during deactivation of three-way catalytic converters on vehicles. *Catal. Today* 63, 371–378. doi: 10.1016/S0920-5861(00)00481-8
- Aswath, P., Chen, X., Sharma, V., Igartua, M. A., Pagano, F., Binder, W., et al. (2017). *Synergistic Mixtures of Ionic Liquids with Other Ionic Liquids and/or with Ashless Thiophosphates for Antiwear and/or Friction Reduction Applications*. U.S. Patent Number 9,725,669
- Bagi, S., Vyavhare, K., and Aswath, P. B. (2018). Tribological characteristics of greases with and without metallo-organic friction-modifiers. *Tribol. Mater. Surfaces Interfaces* 12, 223–236. doi: 10.1080/17515831.2018.1542790
- Bancroft, G. M., Kasrai, M., Fuller, M., Yin, Z., Fyfe, K., and Tan, K. H. (1997). Mechanisms of tribochemical film formation: stability of tribo- and thermally-generated ZDDP films. *Tribol. Lett.* 3, 47–51. doi: 10.1023/A:1019179610589
- Baş, H., and Karabacak, Y. E. (2014). Investigation of the effects of boron additives on the performance of engine oil. *Tribol. Trans.* 57, 740–748. doi: 10.1080/10402004.2014.909549
- Blanco, D., González, R., Viesca, J. L., Fernández-González, A., Bartolomé, M., and Hernández Battez, A. (2017). Antifricción and antiwear properties of an ionic liquid with fluorine-containing anion used as lubricant additive. *Tribol. Lett.* 65:66. doi: 10.1007/s11249-017-0846-4
- Buwono, H. P., Minami, S., Uemura, K., and Machida, M. (2015). Surface properties of Rh/AlPO<sub>4</sub> catalyst providing high resistance to sulfur and phosphorus poisoning. *Ind. Eng. Chem. Res.* 54, 7233–7240. doi: 10.1021/acs.iecr.5b01720
- Cebe, T., Ahuja, N., Monte, F., Awad, K., Vyavhare, K., Aswath, P., et al. (2020). Novel 3D-printed methacrylated chitosan-laponite nanosilicate composite scaffolds enhance cell growth and biomineral formation in MC3T3 pre-osteoblasts. *J. Mater. Res.* 35, 58–75. doi: 10.1557/jmr.2018.260

ECR data indicated that a shorter incubation time for tribofilm formation is achieved from the beneficial interaction of SB with P\_DEHP. The mechanism of tribofilm formation was examined by running tribotests for 5, 15, and 60 min followed by chemical analysis of tribofilms. XANES analysis using P L-edge revealed that phosphorus is primarily present as FePO<sub>4</sub> and phosphate chain polymerization increases with rubbing time (increase in P L-edge a/c ratio from 5 to 60 min test time). B K-edge spectra revealed the formation of BPO<sub>4</sub> enhanced B<sub>2</sub>O<sub>3</sub> tribofilms for P\_DEHP+SB blends while SB alone forms B<sub>2</sub>O<sub>3</sub> chemistry-based tribofilms. Additionally, B K-edge spectra exhibited that BPO<sub>4</sub> to B<sub>2</sub>O<sub>3</sub> ratio increase with rubbing time suggesting that during the thermo-mechanical shearing action, initial B<sub>2</sub>O<sub>3</sub> tribofilms formed from SB chemically interact with P\_DEHP IL to form BPO<sub>4</sub> in addition to FePO<sub>4</sub>.

## DATA AVAILABILITY STATEMENT

The raw data supporting the conclusions of this article will be made available by the authors, without undue reservation.

## AUTHOR CONTRIBUTIONS

KV, VibS, and VinS designed this research work, conducted the experiments, and wrote the manuscript. AE supported and guided tribological tests and data analysis. PA supervised all aspects of this research work and reviewed the paper. All authors contributed to the article and approved the submitted version.

## ACKNOWLEDGMENTS

Tribological tests were conducted at Argonne National Laboratory. XANES experiments were conducted at the Canadian Light Source, Saskatoon, Saskatchewan, Canada that was supported by NSERC, NRC, CIHR, and the University of Saskatchewan.

- Deshmukh, P. V., Lovell, M., and Sawyer, W. G. (2005). On the friction and wear performance of boric acid lubricant combinations. *ASME. World Tribol. Congr.* 1, 545–546. doi: 10.1115/WTC2005-63968
- Erdemir, A. (1991). Tribological properties of boric acid and boric-acid-forming surfaces. Part II, mechanisms of formation and self-lubrication films on boron- and boric oxide-containing surfaces. *Lubr. Eng.* 47, 179–183.
- Erdemir, A. (2008). “Boron-based solid nanolubricants and lubrication additives,” in *Nanolubricants*, eds J. M. Martin and N. Ohmae (West Sussex: John Wiley & Sons), 203–223. doi: 10.1002/9780470987711.ch6
- Erdemir, A., Fenske, G. R., and Erck, R. A. (1990). Study of the formation and self-lubrication mechanisms of boric acid films on boric oxide coatings. *Surf. Coat. Technol.* 44, 588–596.
- Erdemir, A., Fenske, G. R., Erck, R. A., Nicholas, F. A., and Busch, D. E. (1991). Tribological properties of boric acid and boric-acid-forming surfaces. Part I, crystal chemistry and mechanism of self-lubrication of boric acid. *Lubr. Eng.* 47, 168–178.
- Forzatti, P., and Lietti, L. (1999). Catalyst Deactivation. *Catal. Today* 52, 165–181. doi: 10.1016/S0920-5861(99)00074-7
- García, A., González, R., Battez, A. H., Viesca, J. L., Monge, R., Fernández-González, A., et al. (2014). Ionic liquids as a neat lubricant applied to steel–steel contacts. *Tribol. Int.* 72, 42–50. doi: 10.1016/j.triboint.2013.12.007
- González, R., Bartolomé, M., Blanco, D., Viesca, J. L., Fernández-González, A., and Battez, A. H. (2016). Effectiveness of phosphonium cation-based ionic liquids as lubricant additive. *Tribol. Int.* 98, 82–93. doi: 10.1016/j.triboint.2016.02.016
- Greco, A., Mistry, K., Sista, V., Eryilmaz, O., and Erdemir, A. (2011). Friction and wear behaviour of boron based surface treatment and nano-particle lubricant additives for wind turbine gearbox applications. *Wear* 271, 1754–1760. doi: 10.1016/j.wear.2010.11.060
- Huang, G., Yu, Q., Ma, Z., Cai, M., Zhou, F., and Liu, W. (2017). Oil-soluble ionic liquids as antiwear and extreme pressure additives in poly- $\alpha$ -olefin for steel/steel contacts. *Friction* 7, 18–31. doi: 10.1007/s40544-017-0180-8
- Jiménez, A.-E., and Bermúdez, M.-D. (2007). Ionic liquids as lubricants for steel–aluminum contacts at low and elevated temperatures. *Tribol. Lett.* 26, 53–60. doi: 10.1007/s11249-006-9182-9
- Jiménez, A.-E., and Bermúdez, M.-D. (2008). Imidazolium ionic liquids as additives of the synthetic ester propylene glycol dioleate in aluminium–steel lubrication. *Wear* 265, 787–798. doi: 10.1016/j.wear.2008.01.009
- Jiménez, A. E., Bermúdez, M. D., Iglesias, P., Carrión, F. J., and Martínez-Nicolás, G. (2006). 1-N-alkyl-3-methylimidazolium ionic liquids as neat lubricants and lubricant additives in steel–aluminium contacts. *Wear* 260, 766–782. doi: 10.1016/j.wear.2005.04.016
- Khare, H. S., Lahouij, I., Jackson, A., Feng, G., Chen, Z., Cooper, G. D., et al. (2018). Nanoscale generation of robust solid films from liquid-dispersed nanoparticles via *in situ* atomic force microscopy: growth kinetics and nanomechanical properties. *ACS Appl. Mater. Interfaces* 10, 40335–40347. doi: 10.1021/acsami.8b16680
- Kim, B., Jiang, J. C., and Aswath, P. B. (2011). Mechanism of wear at extreme load and boundary conditions with ashless anti-wear additives: analysis of wear surfaces and wear debris. *Wear* 270, 181–194. doi: 10.1016/j.wear.2010.10.058
- Kim, B., Mourhatch, R., and Aswath, P. B. (2010). Properties of tribofilms formed with ashless dithiophosphate and zinc dialkyl dithiophosphate under extreme pressure conditions. *Wear* 268, 579–591. doi: 10.1016/j.wear.2009.10.004
- Kim, B., Sharma, V., and Aswath, P. B. (2017). Chemical and mechanistic interpretation of thermal films formed by dithiophosphates using XANES. *Tribol. Int.* 114, 15–26. doi: 10.1016/j.triboint.2017.04.014
- Kondo, Y., Yagi, S., Koyama, T., Tsuboi, R., and Sasaki, S. (2012). Lubricity and corrosiveness of ionic liquids for steel-on-steel sliding contacts. *Proc. Inst. Mech. Eng. Part J J. Eng. Tribol.* 226, 991–1006. doi: 10.1177/1350650112456127
- Koskilinna, J., Linnolahti, M., and Pakkanen, T. (2006). Friction coefficient for hexagonal boron nitride surfaces from ab initio calculations. *Tribol. Lett.* 24, 37–41. doi: 10.1007/s11249-006-9120-x
- Kröger, V., Lassi, U., Kynkäänniemi, K., Suopanki, A., and Keiski, R. L. (2006). Methodology development for laboratory-scale exhaust gas catalyst studies on phosphorus poisoning. *Chem. Eng. J.* 120, 113–118. doi: 10.1016/j.cej.2006.03.012
- Li, D., Bancroft, G. M., Kasrai, M., Fleet, M. E., Feng, X. H., and Tan, K. H. (1994). High-resolution Si and P K- and L-edge XANES spectra of crystalline SiP<sub>2</sub>O<sub>7</sub> and amorphous SiO<sub>2</sub>-P<sub>2</sub>O<sub>5</sub>. *Am. Mineral.* 79, 785–788.
- Li, Y., Zhang, S., Ding, Q., Li, H., Qin, B., and Hu, L. (2018). Understanding the synergistic lubrication effect of 2-mercaptobenzothiazolate based ionic liquids and Mo nanoparticles as hybrid additives. *Tribol. Int.* 125, 39–45. doi: 10.1016/j.triboint.2018.04.019
- Li, Y. R., Pereira, G., Kasrai, M., and Norton, P. R. (2007). Studies on ZDDP anti-wear films formed under different conditions by XANES spectroscopy, atomic force microscopy and <sup>31</sup>P NMR. *Tribol. Lett.* 28:319. doi: 10.1007/s11249-007-9275-0
- Liang, H., and Jahanmir, S. (1995). Boric acid as an additive for core-drilling of alumina. *J. Tribol.* 117, 65–73.
- Lovell, M. R., Kabir, M. A., Menezes, P. L., and Higgs, C. F. III. (2010). Influence of boric acid additive size on green. *Philos. Trans. R. Soc. A Math. Phys. Eng. Sci.* 368, 4851–4868. doi: 10.1098/rsta.2010.0183
- Lu, Q., Wang, H., Ye, C., Liu, W., and Xue, Q. (2004). Room temperature ionic liquid 1-ethyl-3-hexylimidazolium-bis(trifluoromethylsulfonyl)-imide as lubricant for steel–steel contact. *Tribol. Int.* 37, 547–552. doi: 10.1016/j.triboint.2003.12.003
- Martin, J.M., Le Mogne, T., Chassagnette, C., and Gardos, M. N. (1992). Friction of hexagonal boron nitride in various environments. *Tribol. Trans.* 35, 462–472.
- Miller, B. P., Kotvis, P. V., Furlong, O. J., and Tysoe, W. T. (2012). Relating molecular structure to tribological chemistry: borate esters on copper. *Tribol. Lett.* 49, 21–29. doi: 10.1007/s11249-012-0038-1
- Monge, R., González, R., Battez, A. H., Fernández-González, A., Viesca, J. L., García, A., et al. (2015). Ionic liquids as an additive in fully formulated wind turbine gearbox oils. *Wear* 328–329, 50–63. doi: 10.1016/j.wear.2015.01.041
- Mosey, N. J., Woo, T. K., Kasrai, M., Norton, P. R., Bancroft, G. M., and Müser, M. H. (2006). Interpretation of experiments on ZDDP anti-wear films through pressure-induced cross-linking. *Tribol. Lett.* 24, 105–114. doi: 10.1007/s11249-006-9040-9
- Mosuang, T.E., and Lowther, J. (2002). Relative stability of cubic and different hexagonal forms of boron nitride. *J. Phys. Chem. Solids* 63, 363–368. doi: 10.1016/S0022-3697(00)00254-7
- Mourhatch, R., and Aswath, P. B. (2011). Tribological behavior and nature of tribofilms generated from fluorinated ZDDP in comparison to ZDDP under extreme pressure conditions—part II: morphology and nanoscale properties of tribofilms. *Tribol. Int.* 44, 201–210. doi: 10.1016/j.triboint.2010.10.035
- Mourhatch, R. A. P. (2009). Nanoscale properties of tribofilms formed with zinc dialkyl dithiophosphate (ZDDP) under extreme pressure condition. *J. Nanosci. Nanotechnol.* 9, 2682–2691. doi: 10.1166/jnn.2009.458
- Mu, Z., Wang, X., Zhang, S., Liang, Y., Bao, M., and Liu, W. (2008). Investigation of tribological behavior of Al–Si alloy against steel lubricated with ionic liquids of 1-diethylphosphonyl-n-propyl-3-alkylimidazolium tetrafluoroborate. *ASME. J. Tribol.* 130, 034501–034505. doi: 10.1115/1.2913553
- Mu, Z., Zhou, F., Zhang, S., Liang, Y., and Liu, W. (2005). Effect of the functional groups in ionic liquid molecules on the friction and wear behavior of aluminum alloy in lubricated aluminum-on-steel contact. *Tribol. Int.* 38, 725–731. doi: 10.1016/j.triboint.2004.10.003
- Nicholls, M., Najman, M. N., Zhang, Z., Kasrai, M., Norton, P. R., and Gilbert, P. U. P. A. (2007). The contribution of XANES spectroscopy to tribology. *Can. J. Chem.* 85, 816–830. doi: 10.1139/v07-093
- Philippon, D., De Barros-Bouchet, M. I., Lerasle, O., Le Mogne, T. H., and, T., Martin, J.-M. (2011). Experimental simulation of tribochemical reactions between borates esters and steel surface. *Tribol. Lett.* 41, 73–82. doi: 10.1007/s11249-010-9685-2
- Phillips, B. S., and Zabinski, J. S. (2004). Ionic liquid lubrication effects on ceramics in a water environment. *Tribol. Lett.* 17, 533–541. doi: 10.1023/B:TRIL.0000044501.64351.68
- Qu, J., Bansal, D. G., Yu, B., Howe, J. Y., Luo, H., Dai, S., et al. (2012). Antiwear performance and mechanism of an oil-miscible ionic liquid as a lubricant additive. *ACS Appl. Mater. Interfaces* 4, 997–1002. doi: 10.1021/am201646k
- Qu, J., Barnhill, W. C., Luo, H., Meyer, H. M., Leonard, D. N., and Landauer, A. K. (2015). Synergistic effects between phosphonium-alkylphosphate ionic liquids and Zinc Dialkyl dithiophosphate (ZDDP) as lubricant additives. *Adv. Mater.* 27, 4767–4774. doi: 10.1002/adma.201502037
- Qu, J., Luo, H., Chi, M., Ma, C., Blau, P. J., Dai, S., et al. (2014). Comparison of an oil-miscible ionic liquid and ZDDP as a lubricant anti-wear additive. *Tribol. Int.* 71, 88–97. doi: 10.1016/j.triboint.2013.11.010

- Reeves, C., Menezes, P. L., Lovell, M. R., and Jen, T.-C. (2013). The size effect of boron nitride particles on the tribological performance of biolubricants for energy conservation and sustainability. *Tribol. Lett.* 51, 437–452. doi: 10.1007/s11249-013-0182-2
- Rokosz, M. J., Chen, A. E., Lowe-Ma, C. K., Kucherov, A. V., Benson, D., Paputa Peck, M. C., et al. (2001). Characterization of phosphorus-poisoned automotive exhaust catalysts. *Appl. Catal. B Environ.* 33, 205–215. doi: 10.1016/S0926-3373(01)00165-5
- Shah, F. U., Glavatskih, S., and Antzutkin, N. A. (2013). Boron in tribology: from borates to ionic liquids. *Tribol. Lett.* 51, 281–301. doi: 10.1007/s11249-013-0181-3
- Sharma, V., Doerr, N., and Aswath, P. B. (2016a). Chemical–mechanical properties of tribofilms and their relationship to ionic liquid chemistry. *RSC Adv.* 6, 22341–22356. doi: 10.1039/C6RA01915C
- Sharma, V., Doerr, N., Erdemir, A., and Aswath, P. B. (2016b). Interaction of phosphonium ionic liquids with borate esters at tribological interfaces. *RSC Adv.* 6, 53148–53161. doi: 10.1039/c6ra11822d
- Sharma, V., Dörr, N., Erdemir, A., and Aswath, P. B. (2019a). Antiwear properties of binary ashless blend of phosphonium ionic liquids and borate esters in partially formulated oil (No Zn). *Tribol. Lett.* 67:42. doi: 10.1007/s11249-019-1152-0
- Sharma, V., Gabler, C., Doerr, N., and Aswath, P. B. (2015). Mechanism of tribofilm formation with P and S containing ionic liquids. *Tribol. Int.* 92, 353–364. doi: 10.1016/j.triboint.2015.07.009
- Sharma, V., Johansson, J., Timmons, R. B., Prakash, B., and Aswath, P. B. (2018). Tribological interaction of plasma-functionalized polytetrafluoroethylene nanoparticles with ZDDP and ionic liquids. *Tribol. Lett.* 66:107. doi: 10.1007/s11249-018-1060-8
- Sharma, V., Timmons, R. B., Erdemir, A., and Aswath, P. B. (2019b). Interaction of plasma functionalized TiO<sub>2</sub> nanoparticles and ZDDP on friction and wear under boundary lubrication. *Appl. Surf. Sci.* 489, 372–383. doi: 10.1016/j.apsusc.2019.05.359
- Somers, A. E., Khemchandani, B., Howlett, P. C., Sun, J., Macfarlane, D. R., and Forsyth, M. (2013). Ionic liquids as antiwear additives in base oils: influence of structure on miscibility and antiwear performance for steel on aluminum. *ACS Appl. Mater. Interfaces* 5, 11544–11553. doi: 10.1021/am4037614
- Spikes, H. A. (2004). The history and mechanisms of ZDDP. *Tribol. Lett.* 17, 469–489. doi: 10.1023/B:TRIL.0000044495.26882.b5
- Suominen Fuller, M. L., Rodriguez Fernandez, L., Massoumi, G. R., Lennard, W. N., Kasrai, M., and Bancroft, G. M. (2000). The use of X-ray absorption spectroscopy for monitoring the thickness of antiwear films from ZDDP. *Tribol. Lett.* 8:187. doi: 10.1023/A:1019195404055
- Vyavhare, K., and Aswath, P. B. (2019). Tribological properties of novel multi-walled carbon nanotubes and phosphorus containing ionic liquid hybrids in grease. *Front. Mech. Eng.* 5:15. doi: 10.3389/fmech.2019.00015
- Vyavhare, K., Bagi, S., Patel, M., and Aswath, P. B. (2019). Impact of diesel engine oil additives–soot interactions on physiochemical, oxidation, and wear characteristics of soot. *Energy Fuels* 33, 4515–4530. doi: 10.1021/acs.energyfuels.8b03841
- Vyavhare, K., Bagi, S., Pichumani, P. S., Sharma, V., and Aswath, P. B. (2021a). Chemical and physical properties of tribofilms formed by the interaction of ashless dithiophosphate anti-wear additives. *Lubr. Sci.* doi: 10.1002/lis.1537. [Epub ahead of print].
- Vyavhare, K., Timmons, R. B., Erdemir, A., Edwards, B. L., and Aswath, P. B. (2021b). Robust interfacial tribofilms by borate- and polymer-coated ZnO nanoparticles leading to improved wear protection under a boundary lubrication regime. *Langmuir* 37, 1743–1759. doi: 10.1021/acs.langmuir.0c02985
- Vyavhare, K., Timmons, R. B., Erdemir, A., Edwards, B. L., and Aswath, P. B. (2021c). Tribochemistry of fluorinated ZnO nanoparticles and ZDDP lubricated interface and implications for enhanced anti-wear performance at boundary lubricated contacts. *Wear* 474–475, 203717. doi: 10.1016/j.wear.2021.203717
- Vyavhare, K. P., Timmons, R. B., Erdemir, A., and Aswath, P. B. (2021). Tribological interaction of plasma functionalized CaCO<sub>3</sub> nanoparticles with zinc and ashless dithiophosphate additives. *Tribol. Lett.* Preprint. doi: 10.21203/rs.3.rs-210447/v1
- Watanabe, S., Miyake, S., and Murakawa, M. (1991). Tribological properties of cubic, amorphous and hexagonal boron nitride films. *Surf. Coat. Technol.* 49, 406–410.
- Weng, L. J., Liu, X. Q., Liang, Y. M., and Xue, Q. J. (2007). Effect of tetraalkylphosphonium based ionic liquids as lubricants on the tribological performance of a steel-on-steel system. *Tribol. Lett.* 26, 11–17. doi: 10.1007/s11249-006-9175-8
- Williamson, W. B., Perry, J., Gandhi, H. S., and Bomback, J. L. (1985). Effects of oil phosphorus on deactivation of monolithic three-way catalysts. *Appl. Catal.* 15, 277–292. doi: 10.1016/S0166-9834(00)81842-4
- Xia, Y., Wang, S., Zhou, F., Wang, H., Lin, Y., and Xu, T. (2006). Tribological properties of plasma nitrided stainless steel against SAE52100 steel under ionic liquid lubrication condition. *Tribol. Int.* 39, 635–640. doi: 10.1016/j.triboint.2005.04.030
- Ye, C., Liu, W., Chen, Y., and Yu, L. (2001). Room-temperature ionic liquids: a novel versatile lubricant. *Chem. Commun.* 21, 2244–2245. doi: 10.1039/B106935G
- Yin, Z., Kasrai, M., Bancroft, G. M., Tan, K. H., and Feng, X. (1995). X-ray-absorption spectroscopic studies of sodium polyphosphate glasses. *Phys. Rev. B* 51:742.
- Yu, B., Bansal, D. G., Qu, J., Sun, X., Luo, H., Dai, S., et al. (2012). Oil-miscible and non-corrosive phosphonium-based ionic liquids as candidate lubricant additives. *Wear* 289, 58–64. doi: 10.1016/j.wear.2012.04.015
- Zhang, Y., Cai, T., Shang, W., Sun, L., Liu, D., Tong, D., et al. (2017). Environmental friendly polyisobutylene-based ionic liquid containing chelated orthoborate as lubricant additive: synthesis, tribological properties and synergistic interactions with ZDDP in hydrocarbon oils. *Tribol. Int.* 115, 297–306. doi: 10.1016/j.triboint.2017.05.038
- Zhang, Z., Yamaguchi, E. S., Kasrai, M., and Bancroft, G. M. (2004). Interaction of ZDDP with borated dispersant using XANES and XPS. *Tribol. Trans.* 47, 527–536. doi: 10.1080/05698190490500725
- Zheng, Z., Shen, G., Wan, Y., Cao, L., Xu, X., Yue, Q., et al. (1998). Synthesis, hydrolytic stability and tribological properties of novel borate esters containing nitrogen as lubricant additives. *Wear* 222, 135–144.
- Zhou, Y., Graham, T. W., Luo, H., Leonard, D. N., and Qu, J. (2014). Ionic liquids composed of phosphonium cations and organophosphate, carboxylate, and sulfonate anions as lubricant antiwear additives. *Langmuir* 30, 13301–13311. doi: 10.1021/la5032366
- Zhou, Y., Leonard, D. N., Guo, W., and Qu, J. (2017). Understanding tribofilm formation mechanisms in ionic liquid lubrication. *Sci. Rep.* 7:8426. doi: 10.1038/s41598-017-09029-z

**Conflict of Interest:** The authors declare that the research was conducted in the absence of any commercial or financial relationships that could be construed as a potential conflict of interest.

Copyright © 2021 Vyavhare, Sharma, Sharma, Erdemir and Aswath. This is an open-access article distributed under the terms of the Creative Commons Attribution License (CC BY). The use, distribution or reproduction in other forums is permitted, provided the original author(s) and the copyright owner(s) are credited and that the original publication in this journal is cited, in accordance with accepted academic practice. No use, distribution or reproduction is permitted which does not comply with these terms.